research communications

Chiral *versus* achiral crystal structures of 4-benzyl-1*H*-pyrazole and its 3,5-diamino derivative

Emily R. Hayward,[a] Matthias Zeller[b] and Gellert Mezei[a]*

[a]Western Michigan University, Department of Chemistry, 1903 W. Michigan Ave., Kalamazoo, MI 49008, USA, and [b]Department of Chemistry, Purdue University, 560 Oval Dr., West Lafayette, IN 47907, USA. *Correspondence e-mail: gellert.mezei@wmich.edu
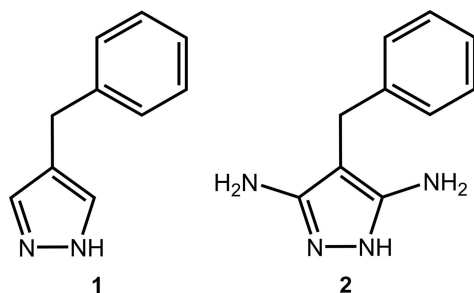
The crystal structures of 4-benzyl-1*H*-pyrazole ($C_{10}H_{10}N_2$, **1**) and 3,5-diamino-4-benzyl-1*H*-pyrazole ($C_{10}H_{12}N_4$, **2**) were measured at 150 K. Although its different conformers and atropenantiomers easily interconvert in solution by annular tautomerism and/or rotation of the benzyl substituent around the C(pyrazole)—C(CH$_2$) single bond (as revealed by ^{1}H NMR spectroscopy), **1** crystallizes in the non-centrosymmetric space group $P2_1$. Within its crystal structure, the pyrazole and phenyl aromatic moieties are organized into alternating bilayers. Both pyrazole and phenyl layers consist of aromatic rings stacked into columns in two orthogonal directions. Within the pyrazole layer, the pyrazole rings form parallel catemers by N—H···N hydrogen bonding. Compound **2** adopts a similar bilayer structure, albeit in the centrosymmetric space group $P2_1/c$, with pyrazole N—H protons as donors in N—H···π hydrogen bonds with neighboring pyrazole rings, and NH$_2$ protons as donors in N—H···N hydrogen bonds with adjacent pyrazoles and other NH$_2$ moieties. The crystal structures and supramolecular features of **1** and **2** are contrasted with the two known structures of their analogs, 3,5-dimethyl-4-benzyl-1*H*-pyrazole and 3,5-diphenyl-4-benzyl-1*H*-pyrazole.

1. Chemical context

1*H*-Pyrazole (pzH) is a chemically and thermally robust organic molecule (Katritzky *et al.*, 2010). Hence, its functionalized derivatives have found widespread applications as pharmaceuticals, pesticides and dyes (Ahmed *et al.*, 2016 and references therein). Owing to its adjacent pair of N atoms, pyrazole derivatives are also very popular in coordination chemistry, especially for the construction of discrete polynuclear complexes (Al Isawi *et al.*, 2021 and references therein). Within the crystal packing of pyrazole derivatives with different substituents, N—H···N hydrogen bonding between pz moieties leads to either discrete hydrogen-bonded motifs, such as dimers, trimers, tetramers and hexamers, or polymeric catemers depending on the substituents (Alkorta *et al.*, 2006; Bertolasi *et al.*, 1999; Cammers & Parkin, 2004; Claramunt *et al.*, 2006; Foces-Foces *et al.*, 2000). In general, the overall crystal structure is the result of the interplay of optimal shape packing and multiple different intermolecular forces, including electrostatic interactions, hydrophobic effects, aromatic interactions, hydrogen bonding with potential hydrogen-bond donor/acceptor substituents, halogen bonding and other non-covalent interactions.

Figure 2
Displacement ellipsoid plot (50% probability) of the crystal structure of 3,5-diamino-4-benzyl-1*H*-pyrazole (**2**), showing the contents of the asymmetric unit.
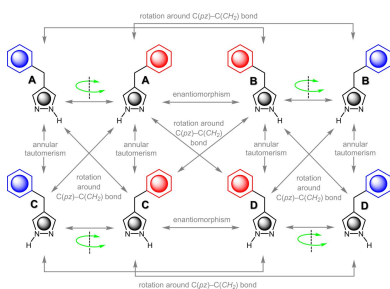
2. Structural commentary

Displacement ellipsoid plots of the crystal structures of **1** and **2** are shown in Figs. 1 and 2, respectively. Similarly to the parent pyrazole (La Cour & Rasmussen, 1973; Sikora & Katrusiak, 2013) and 4-fluoropyrazole (Ahmed *et al.*, 2023), the NH and N centers of the pz rings in **1** and **2** are not disordered and two distinct sets of C—N and C—C bond distances are observed. Thus, the C—N bond adjacent to N is shorter than the one adjacent to NH, whereas the C—C bond adjacent to N is longer than the one adjacent to NH (see supporting information). This is in contrast with other pyrazole derivatives, such as 4-phenylpyrazole (Reger *et al.*, 2003) and 4-halopyrazoles (halogen = Cl, Br, I; Rue & Raptis, 2021; Foces-Foces *et al.*, 1999; Rue *et al.*, 2023), where the N—H hydrogen atom is disordered over the two N atoms of the pyrazole unit. Otherwise, the N—N, C—N and C—C bond lengths in **1** and **2** are similar to those observed in related pyrazole derivatives. C—C—C bond angles between the pz, CH_2 and Ph units are 63.85 (15)° in **1** and 65.65 (9)° in **2**, with pz/Ph centroid–centroid distances of 4.8294 (10) and 4.7376 (9) Å, respectively. While the dihedral angles between the pz and Ph units
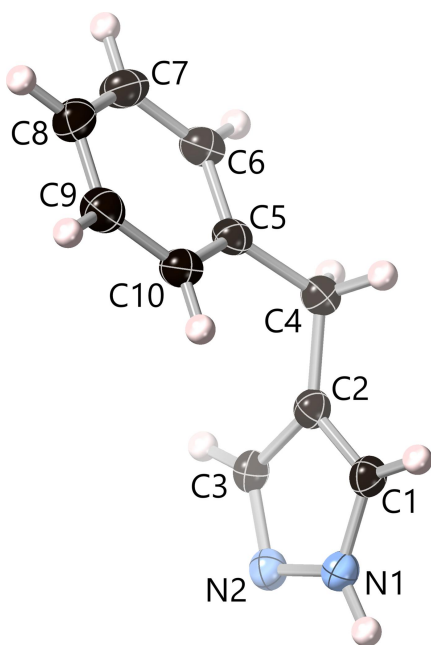
in **1** and **2** are not very disparate [86.00 (7) and 65.27 (4)°], the corresponding individual fold and twist angles are rather different. Specifically, the fold angle is much smaller in **1** [17.52 (12)°] than in **2** [76.12 (8)°], whereas the twist angle is much larger in **1** [65.00 (4)°] than in **2** [7.42 (6)°].

An interesting difference between the structures of **1** ($P2_1$) and **2** ($P2_1/c$) is related to their crystal symmetry. Although 4-benzyl-1*H*-pyrazole displays axial chirality (atropisomerism; Basilaia *et al.*, 2022) in the crystal structure described here, the two atropenantiomers can interconvert in solution by rotation of the benzyl substituent around the C(pz)—C(CH_2) single bond (Fig. 3). Even if the direct conversion of conformer **A** to conformer **B** by rotation of the benzyl group from one side to

Figure 1
Displacement ellipsoid plot (50% probability) of the crystal structure of 4-benzyl-1*H*-pyrazole (**1**), showing the contents of the asymmetric unit.
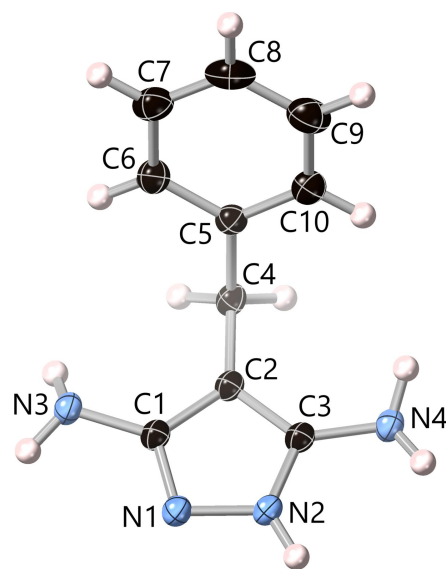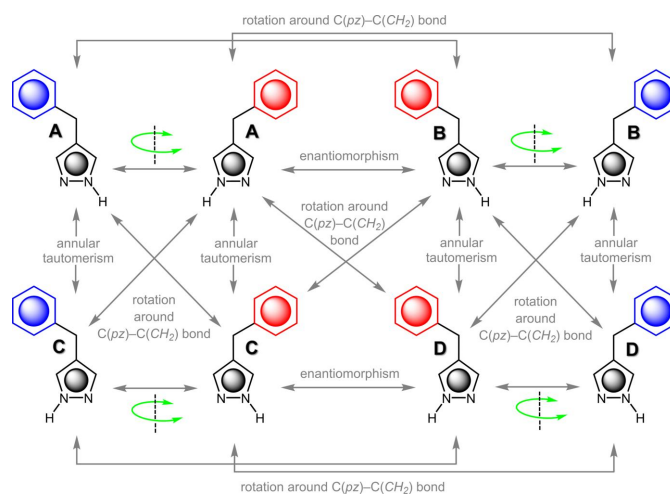

Figure 3
Interconversion between the different conformers, tautomers and atropenantiomers of 4-benzyl-1*H*-pyrazole (**A–D**) by annular tautomerism and/or rotation of the benzyl moiety (red: *above* pz plane; blue: *below* pz plane) around the C—C bond between the pz and CH_2 units.
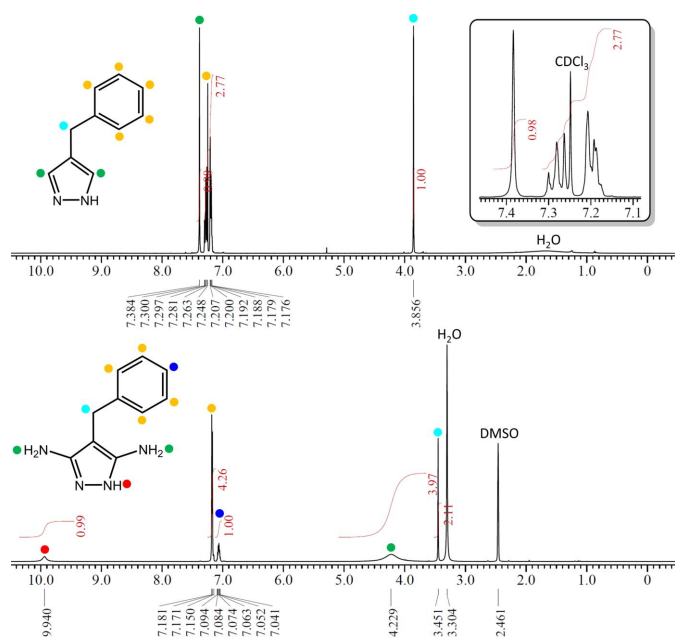
Figure 4
^{1}H NMR spectra of **1** in CDCl$_3$ (upper) and **2** in DMSO-d_6 (lower) at ambient temperature. The signal for the NH proton of **1** is not detectable due to exchange with the solvent deuterium.

the other side of the pz moiety would meet a significant barrier (caused by bulky substituents on the pz ring), **A** can still convert to **B** through its annular tautomer **C**. The latter converts to **B** by a same-side rotation of the benzyl group. Despite the facile interconversion of its different conformers (**A–D**), evidenced by a single resonance for the two pyrazole C—H protons in its ^{1}H NMR spectrum (Fig. 4), **1** adopts a chiral crystal structure (in the achiral, yet non-centrosymmetric space group $P2_1$; Flack, 2003). This must be the result of a more efficient crystal packing in the non-centrosymmetric space group (detailed in the next section) than in a centrosymmetric one.

3. Supramolecular features

The pz moieties in **1** are organized into layers along the *ab* plane, which consist of two symmetry-related (by a 2_1 screw axis) halves (Fig. 5). Within each half, the pz moieties are all parallel to each other (crystallographically imposed) and are organized into parallel columns along both the *a* and *b* axes (which are orthogonal), with pz–pz interplanar distances of 3.540 (4) and 2.184 (5) Å, and centroid–centroid distances of 5.6651 (5) and 5.7566 (6) Å, respectively. The two halves of the pz layer are connected by edge-to-face pz–pz interactions with dihedral angles of 44.59 (11)° and centroid–centroid distances of 4.3813 (12) Å (closest H···pz-plane and H···pz-centroid distances: 2.7021 (8) and 2.7052 (8) Å), as well as by N—H···N hydrogen bonding between pz moieties (Table 1), which leads to catemers along the *b* axis with pz/pz dihedral angles of 44.59 (11)° and centroid–centroid distances of 4.3813 (12) Å).

Table 1
Hydrogen-bond geometry (Å, °) for **1**.

D—H···A	D—H	H···A	D···A	D—H···A
N1—H1N···N2^{i}	0.90 (2)	2.01 (2)	2.887 (2)	163 (2)

Symmetry code: (i) $-x, y - \frac{1}{2}, -z + 1$.

Similarly to the pz moieties, the phenyl moieties of **1** also form layers along the *ab* plane, with two 2_1 screw axis-related halves comprised of parallel columns along both the *a* and *b* axes [Ph–Ph interplanar distances of 2.557 (4) and 3.516 (4) Å, and centroid–centroid distances of 5.6651 (5) and 5.7566 (6) Å, respectively]. Edge-to-face Ph–Ph interactions connect the two halves of the Ph layer, with dihedral angles of 75.29 (9)° and centroid–centroid distances of 4.8833 (11) Å [closest H···Ph-plane and H···Ph-centroid distances: 2.7962 (10) and 2.8660 (7) Å].

The benzyl protons of **1** are involved in C—H···π hydrogen bonding with neighboring pz and Ph moieties, with H···pz/Ph-plane, H···pz/Ph-centroid and closest H···N/C distances of 2.6778 (16), 3.1016 (8), 2.7399 (17), and 2.503 (2), 3.3598 (9), 2.659 (2) Å, respectively.

In **2**, the pz moieties form layers along the *bc* plane, which are comprised of two 2_1 screw axis-related halves as in **1** (Fig. 6). Here, however, the pz moieties are only parallel within individual columns and in every second column, with dihedral angles between neighboring inter-columnar pz moieties of 85.71 (7)° [centroid–centroid distance: 5.9674 (8) Å]. Within each column, the pz–pz interplanar and centroid–centroid distances are 3.4653 (18) and 4.7271 (7) Å, respectively. The two halves of the pz layer are connected by
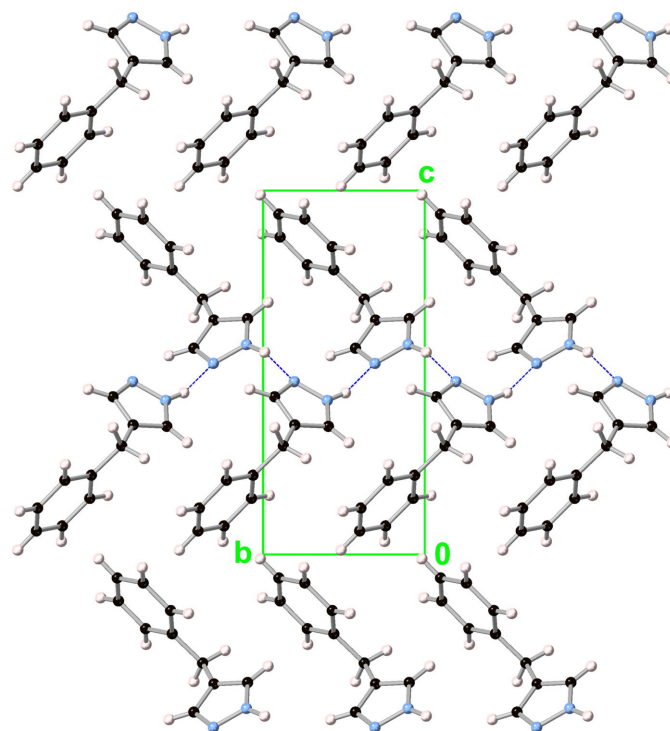

Figure 5
Packing diagram (viewed along the *a* axis) of 4-benzyl-1*H*-pyrazole (**1**).

Table 2
Hydrogen-bond geometry (Å, °) for **2**.

D—H$\cdots A$	D—H	H$\cdots A$	$D\cdots A$	D—H$\cdots A$
N2—H2$\cdots$N1^{i}	0.894 (16)	2.108 (16)	2.9912 (13)	169.7 (14)
N3—H3$A\cdots$N1^{ii}	0.898 (17)	2.240 (17)	3.1032 (14)	161.0 (13)
N3—H3$B\cdots$N4^{iii}	0.905 (17)	2.383 (16)	3.1521 (14)	142.8 (13)
N4—H4$A\cdots$N3^{iv}	0.905 (17)	2.140 (18)	3.0388 (14)	171.7 (14)

Symmetry codes: (i) $-x + 1, y + \frac{1}{2}, -z + \frac{1}{2}$; (ii) $-x + 1, -y + 1, -z + 1$; (iii) $x, -y + \frac{1}{2}, z + \frac{1}{2}$; (iv) $x, -y + \frac{3}{2}, z - \frac{1}{2}$.

edge-to-face interactions characterized by dihedral angles of 85.71 (7)° and centroid–centroid distances of 4.5404 (9) Å [closest H$\cdots$pz-plane, H$\cdots$pz-centroid and H$\cdots$N distances: 1.974 (16), 2.769 (16) and 2.108 (16) Å], as well as by N—H$\cdots$N hydrogen bonding (Table 2). Unlike in **1**, this inter-layer hydrogen bonding in **2** occurs between NH$_2$ donor and N(pz) acceptor moieties, while the N—H(pz) hydrogen atom is involved in an N—H$\cdots\pi$ interaction. Within each half-layer, there are additional hydrogen bonds between neighboring NH$_2$ groups, one on each side of the pz moieties (Table 2). Since there are five N—H hydrogen-bond donors but only four hydrogen-bond acceptors in **2**, one of the NH$_2$ hydrogen atoms does not have a hydrogen-bond acceptor. Instead, an N—H$\cdots\pi$ interaction is formed with a neighboring Ph moiety, with H$\cdots$Ph-plane, H$\cdots$Ph-centroid and closest H$\cdots$C distances of 2.840 (15), 3.363 (15) and 2.956 (15) Å, respectively.
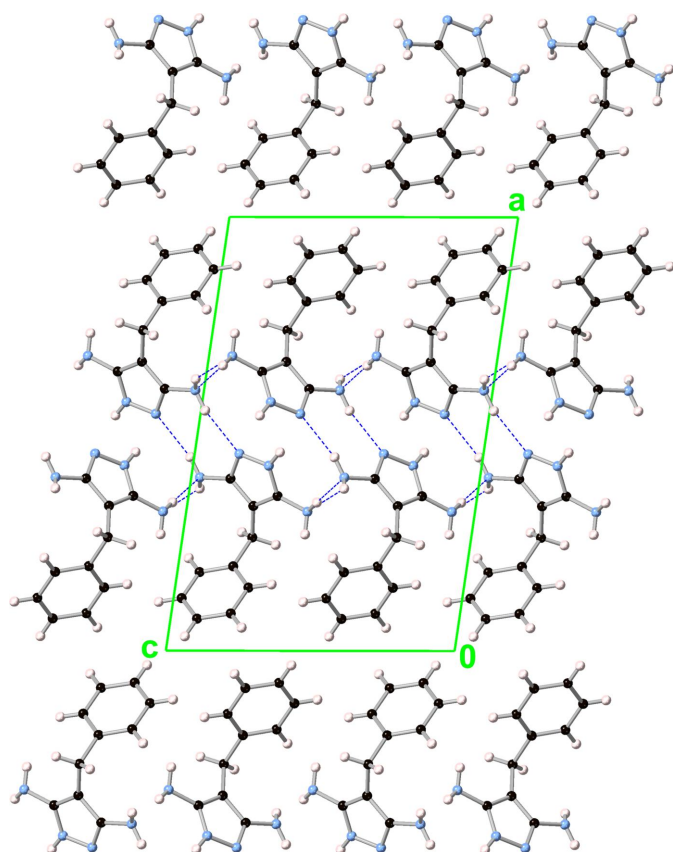

Figure 6
Packing diagram (viewed along the *b* axis) of 3,5-diamino-4-benzyl-1*H*-pyrazole (**2**).

Similarly to **1**, the phenyl moieties of **2** form layers but along the *bc* plane, which are analogous to the layers formed by its pz moieties with dihedral angles of 85.07 (6)° between neighboring inter-columnar Ph moieties [centroid–centroid distance: 6.0946 (8) Å]. Within each column, the Ph–Ph interplanar and centroid–centroid distances are 3.4833 (18) and 4.7271 (7) Å, respectively. Because the Ph moieties in neighboring columns are not parallel, two types of Ph–Ph interactions are present between the two halves of the Ph layer. Edge-to-face interactions are characterized by dihedral angles of 85.07 (6)° and centroid–centroid distances of 5.4925 (10) Å [closest H$\cdots$Ph-plane and H$\cdots$Ph-centroid distances: 2.8014 (3) and 3.4126 (6) Å], in addition to offset stacked interactions between parallel Ph moieties with interplanar and centroid–centroid distances of 1.997 (3) and 6.0466 (13) Å, respectively.

In **2**, only one of the benzyl protons is involved in C—H$\cdots\pi$ hydrogen bonding with neighboring pz moieties, characterized by H$\cdots$pz-plane, H$\cdots$pz-centroid and closest H$\cdots$C distances of 2.9081 (9), 3.2096 (5) and 2.9183 (11) Å, respectively.

4. Database survey

Two crystal structures of simple derivatives of 4-benzyl-1*H*-pyrazole are known, namely 3,5-dimethyl-4-benzyl-1*H*-pyrazole (**3**; Wang & Kong, 2011; CCDC refcode: OBUHOK) and 3,5-diphenyl-4-benzyl-1*H*-pyrazole (**4**; Huang *et al.*, 2007; CCDC refcode: XEYYAC). Interestingly, 3,5-dimethyl-4-benzyl-1*H*-pyrazole crystallizes in the same space group (*P*2$_1$) as its parent compound, 4-benzyl-1*H*-pyrazole (**1**), instead of the centrosymmetric space group (*P*2$_1$/*c*) of its structurally more similar 3,5-diamino-4-benzyl-1*H*-pyrazole (**2**). This is likely due to the hydrogen-bond donor/acceptor ability of the NH$_2$ groups of **2** compared to the CH$_3$ groups of **3**.

Not only does **3** crystallize in the same space group as **1**, but it also adopts a very similar crystal packing in a unit cell of comparable dimensions [*a* = 6.2303 (6) Å; *b* = 5.5941 (5) Å; *c* = 15.1364 (15) Å; β = 97.049 (1)°]. Notably, its *c* axis is longer than in **1** [13.2321 (9) Å] to accommodate the bulkier CH$_3$ group compared to H. The C—C—C bond angle of 66.3 (3)° between the pz, CH$_2$ and Ph units is closer to that of **2** [65.65 (8)°], with a pz/Ph centroid–centroid distance of 4.6524 (2) Å, shorter than in both **1** and **2**. The dihedral angle of 78.65 (13)° between the pz and Ph units in **3** is in-between the values of **1** and **2**, with individual fold and twist angles of 60.60 (14) and 52.27 (16)°.

The supramolecular features of **3** are similar to those of **1**, with a slightly expanded crystal packing due to the presence of the CH$_3$ groups. Thus, the parallel columns along the *a* and *b* axes feature pz–pz interplanar distances of 2.995 (8) and 3.514 (7) Å, and centroid–centroid distances of 6.2303 (6) and 5.5941 (5) Å, respectively. The edge-to-face orientation of the pz/pz pairs within the two halves of the pz layer is described by a dihedral angle of 77.83 (18)° and centroid–centroid distance of 5.8969 (19) Å, which are significantly larger than the corresponding values in **1** [44.59 (11)° and 4.3813 (12) Å]. The N—H$\cdots$N hydrogen bonding between pz moieties leading to

Table 3
Experimental details.

	1	2
Crystal data		
Chemical formula	$C_{10}H_{10}N_2$	$C_{10}H_{12}N_4$
M_r	158.20	188.24
Crystal system, space group	Monoclinic, $P2_1$	Monoclinic, $P2_1/c$
Temperature (K)	150	150
a, b, c (Å)	5.6651 (5), 5.7566 (6), 13.2321 (9)	17.410 (2), 4.7271 (7), 11.4664 (15)
β (°)	101.732 (4)	98.247 (6)
V (Å^3)	422.51 (6)	933.9 (2)
Z	2	4
Radiation type	Cu $K\alpha$	Cu $K\alpha$
μ (mm^{-1})	0.59	0.69
Crystal size (mm)	$0.14 \times 0.13 \times 0.09$	$0.23 \times 0.21 \times 0.11$
Data collection		
Diffractometer	Bruker AXS D8 Quest	Bruker AXS D8 Quest
Absorption correction	Multi-scan (*SADABS*; Krause *et al.*, 2015)	Multi-scan (*SADABS*; Krause *et al.*, 2015)
T_{min}, T_{max}	0.605, 0.754	0.543, 0.754
No. of measured, independent and observed [$I > 2\sigma(I)$] reflections	4021, 1612, 1549	10090, 1963, 1817
R_{int}	0.052	0.063
$(\sin\theta/\lambda)_{max}$ (Å^{-1})	0.639	0.638
Refinement		
$R[F^2 > 2\sigma(F^2)]$, $wR(F^2)$, S	0.032, 0.084, 1.08	0.038, 0.095, 1.03
No. of reflections	1612	1963
No. of parameters	112	142
No. of restraints	1	0
H-atom treatment	H atoms treated by a mixture of independent and constrained refinement	H atoms treated by a mixture of independent and constrained refinement
$\Delta\rho_{max}$, $\Delta\rho_{min}$ (e Å^{-3})	0.15, −0.16	0.21, −0.20
Absolute structure	Flack x determined using 605 quotients $[(I^+)-(I^-)]/[(I^+)+(I^-)]$ (Parsons *et al.*, 2013)	–
Absolute structure parameter	0.0 (3)	–

Computer programs: *APEX5* (Bruker, 2023), *SAINT* (Bruker, 2020), *SHELXT* (Sheldrick, 2015a), *SHELXL2019/2* (Sheldrick, 2015b), *ShelXle* (Hübschle *et al.*, 2011) and *CrystalMaker* (CrystalMaker Software, 2003).

catemers along the *b* axis is characterized by N—H, H···N and N···N distances of 0.86, 2.09 and 2.946 (4) Å, with an N—H···N angle of 170°, pz/pz dihedral angle of 77.83 (18)° and centroid–centroid distance of 4.9789 (19) Å. The corresponding values for the Ph–Ph interactions along the *a* and *b* axes are 2.202 (11) and 3.772 (7) Å (interplanar) and 6.2302 (6) and 5.5941 (5) Å (centroid–centroid), whereas between the two halves of the Ph layer the values are 84.8 (2)° (dihedral angle) and 5.066 (3) Å (centroid–centroid), with closest H···Ph-plane and H···Ph-centroid distances of 2.863 (3) and 3.1738 (17) Å. Similarly to **1**, the methyl and benzyl protons are involved in various C—H···π interactions with neighboring pz and Ph moieties.

3,5-Diphenyl-4-benzyl-1*H*-pyrazole (**4**) crystallizes in the centrosymmetric space group $P2_1/c$. As opposed to **1**–**3**, however, the N—H···N hydrogen bonding between pz moieties does not lead to catemers. Instead, **4** forms hydrogen-bonded dimers, with an overall crystal packing very different from the ones of **1**–**3**.

5. Synthesis and crystallization

4-Benzyl-1*H*-pyrazole (**1**) was synthesized by reduction with hypophosphorous acid of 3,5-diamino-4-benzyl-1*H*-pyrazole (**2**) (Echevarría & Elguero, 1993), which in turn was obtained from benzylmalononitrile by reaction with hydrazine hydrate

(Vaquero *et al.*, 1987). The synthesis of benzylmalononitrile by alkylation of malononitrile with benzyl bromide provided the monobenzylated product contaminated with large amounts of dibenzylated side product (Díez-Barra *et al.*, 1991). Therefore, an alternate method, by the reaction of malononitrile with benzaldehyde and reduction of the benzylidenemalononitrile intermediate with NaBH$_4$ was used for the preparation of pure benzylmalononitrile in high yield (Tayyari *et al.*, 2008). Single crystals were grown by recrystallization from hot *n*-heptane (**1**) or by vapor diffusion of benzene into a solution in pyridine at room temperature (**2**).

6. Refinement

Crystal data, data collection and structure refinement details are summarized in Table 3. C—H bond distances were constrained to 0.95 Å (pz and Ph) or 0.99 Å (CH$_2$) and refined as riding. Positions of N-bound H atoms were freely refined. U_{iso}(H) values were set to 1.2 or 1.5 times U_{eq}(C/N) for H atoms.

References

Ahmed, B. M., Zeller, M. & Mezei, G. (2023). *Acta Cryst.* E**79**, 428–431.

Ahmed, B. M., Zhang, H., Mo, Y. & Mezei, G. (2016). *J. Org. Chem.* **81**, 1718–1722.

Al Isawi, W. A., Zeller, M. & Mezei, G. (2021). *Inorg. Chem.* **60**, 13479–13492.

Alkorta, I., Elguero, J., Foces-Foces, C. & Infantes, L. (2006). *ARKIVOC* **(ii)**, 15–30.

Basilaia, M., Chen, M. H., Secka, J. & Gustafson, J. L. (2022). *Acc. Chem. Res.* **55**, 2904–2919.

Bertolasi, V., Gilli, P., Ferretti, V., Gilli, G. & Fernàndez-Castaño, C. (1999). *Acta Cryst.* B**55**, 985–993.

Bruker (2020). *SAINT*. Bruker AXS Inc., Madison, Wisconsin, USA.

Bruker (2023). *APEX5*. Bruker AXS Inc., Madison, Wisconsin, USA.

Cammers, A. & Parkin, S. (2004). *CrystEngComm*, **6**, 168–172.

Claramunt, R. M., Cornago, P., Torres, V., Pinilla, E., Torres, M. R., Samat, A., Lokshin, V., Valés, M. & Elguero, J. (2006). *J. Org. Chem.* **71**, 6881–6891.

CrystalMaker Software (2003). *CrystalMaker*. CrystalMaker Software, Bicester, England.

Díez-Barra, E., de la Hoz, A., Moreno, A. & Sánchez-Verdú, P. (1991). *J. Chem. Soc. Perkin Trans. 1*, pp. 2589–2592.

Echevarría, A. & Elguero, J. (1993). *Synth. Commun.* **23**, 925–930.

Flack, H. D. (2003). *Helv. Chim. Acta*, **86**, 905–921.

Foces-Foces, C., Alkorta, I. & Elguero, J. (2000). *Acta Cryst.* B**56**, 1018–1028.

Foces-Foces, C., Llamas-Saiz, A. L. & Elguero, J. (1999). *Z. Kristallogr.* **214**, 237–241.

Huang, H.-P., Wu, Q., Liu, L.-X. & Sun, Q.-F. (2007). *Acta Cryst.* E**63**, o1473–o1474.

Hübschle, C. B., Sheldrick, G. M. & Dittrich, B. (2011). *J. Appl. Cryst.* **44**, 1281–1284.

Katritzky, A. R., Ramsden, C. A., Joule, J. A. & Zhdankin, V. V. (2010). *Handbook of Heterocyclic Chemistry*, 3rd ed. Amsterdam: Elsevier.

Krause, L., Herbst-Irmer, R., Sheldrick, G. M. & Stalke, D. (2015). *J. Appl. Cryst.* **48**, 3–10.

La Cour, T. & Rasmussen, S. E. (1973). *Acta Chem. Scand.* **27**, 1845–1854.

Parsons, S., Flack, H. D. & Wagner, T. (2013). *Acta Cryst.* B**69**, 249–259.

Reger, D. L., Gardinier, J. R., Christian Grattan, T., Smith, M. R. & Smith, M. D. (2003). *New J. Chem.* **27**, 1670–1677.

Rue, K. & Raptis, R. G. (2021). *Acta Cryst.* E**77**, 955–957.

Rue, K. L., Herrera, S., Chakraborty, I., Mebel, A. M. & Raptis, R. G. (2023). *Crystals*, **13**, 1101.

Sheldrick, G. M. (2015a). *Acta Cryst.* A**71**, 3–8.

Sheldrick, G. M. (2015b). *Acta Cryst.* C**71**, 3–8.

Sikora, M. & Katrusiak, A. (2013). *J. Phys. Chem. C*, **117**, 10661–10668.

Tayyari, F., Wood, D. E., Fanwick, P. E. & Sammelson, R. E. (2008). *Synthesis*, pp. 279–285.

Vaquero, J. J., Fuentes, L., Del Castillo, J. C., Pérez, M. I., García, J. L. & Soto, J. L. (1987). *Synthesis*, pp. 33–35.

Wang, S.-Q. & Kong, C. (2011). *Acta Cryst.* E**67**, o3199.

Chiral *versus* achiral crystal structures of 4-benzyl-1*H*-pyrazole and its 3,5-di-amino derivative

Emily R. Hayward, Matthias Zeller and Gellert Mezei

Computing details

4-Benzyl-1*H*-pyrazole (1)

Crystal data

$C_{10}H_{10}N_2$	$F(000) = 168$
$M_r = 158.20$	$D_x = 1.244$ Mg m^{-3}
Monoclinic, $P2_1$	Cu $K\alpha$ radiation, $\lambda = 1.54178$ Å
$a = 5.6651$ (5) Å	Cell parameters from 3320 reflections
$b = 5.7566$ (6) Å	$\theta = 3.4–78.8°$
$c = 13.2321$ (9) Å	$\mu = 0.59$ mm^{-1}
$\beta = 101.732$ (4)°	$T = 150$ K
$V = 422.51$ (6) Å^3	Plate, colourless
$Z = 2$	$0.14 \times 0.13 \times 0.09$ mm

Data collection

Bruker AXS D8 Quest diffractometer	$T_{min} = 0.605$, $T_{max} = 0.754$
Radiation source: I-mu-S 3.0 microsource X-ray tube	4021 measured reflections
	1612 independent reflections
HELIOS multilayer Montel optics monochromator	1549 reflections with $I > 2\sigma(I)$
	$R_{int} = 0.052$
Detector resolution: 7.4074 pixels mm^{-1}	$\theta_{max} = 80.0°$, $\theta_{min} = 3.4°$
ω and phi scans	$h = -6 \rightarrow 5$
Absorption correction: multi-scan (SADABS; Krause *et al.*, 2015)	$k = -6 \rightarrow 7$
	$l = -16 \rightarrow 16$

Refinement

Refinement on F^2	H atoms treated by a mixture of independent and constrained refinement
Least-squares matrix: full	$w = 1/[\sigma^2(F_o^2) + (0.0261P)^2 + 0.0328P]$ where $P = (F_o^2 + 2F_c^2)/3$
$R[F^2 > 2\sigma(F^2)] = 0.032$	
$wR(F^2) = 0.084$	
$S = 1.08$	$(\Delta/\sigma)_{max} < 0.001$
1612 reflections	$\Delta\rho_{max} = 0.14$ e Å^{-3}
112 parameters	$\Delta\rho_{min} = -0.16$ e Å^{-3}
1 restraint	Absolute structure: Flack x determined using 605 quotients $[(I^+)-(I^-)]/[(I^+)+(I^-)]$ (Parsons *et al.*, 2013)
Primary atom site location: dual	
Secondary atom site location: difference Fourier map	Absolute structure parameter: 0.0 (3)
Hydrogen site location: mixed	

Special details

Geometry. All esds (except the esd in the dihedral angle between two l.s. planes) are estimated using the full covariance matrix. The cell esds are taken into account individually in the estimation of esds in distances, angles and torsion angles; correlations between esds in cell parameters are only used when they are defined by crystal symmetry. An approximate (isotropic) treatment of cell esds is used for estimating esds involving l.s. planes.

Fractional atomic coordinates and isotropic or equivalent isotropic displacement parameters (Å^2)

	x	*y*	*z*	U_{iso}*/U_{eq}
N1	0.2067 (3)	0.1035 (3)	0.57682 (11)	0.0298 (3)
H1N	0.097 (4)	−0.009 (4)	0.5558 (18)	0.045*
N2	0.1810 (3)	0.3078 (3)	0.52511 (10)	0.0304 (3)
C1	0.4146 (3)	0.0962 (3)	0.64801 (12)	0.0296 (4)
H1	0.469928	−0.030094	0.692813	0.036*
C2	0.5319 (3)	0.3046 (3)	0.64400 (12)	0.0281 (4)
C3	0.3770 (3)	0.4290 (3)	0.56670 (13)	0.0294 (4)
H3	0.408236	0.582314	0.546294	0.035*
C4	0.7775 (3)	0.3749 (3)	0.70179 (14)	0.0333 (4)
H4A	0.872243	0.428501	0.651089	0.040*
H4B	0.858928	0.235376	0.736236	0.040*
C5	0.7846 (3)	0.5626 (3)	0.78212 (12)	0.0285 (4)
C6	0.9684 (3)	0.7272 (3)	0.79620 (14)	0.0342 (4)
H6	1.083272	0.724351	0.752955	0.041*
C7	0.9862 (4)	0.8950 (4)	0.87229 (15)	0.0413 (5)
H7	1.113464	1.005361	0.881061	0.050*
C8	0.8206 (4)	0.9031 (4)	0.93542 (15)	0.0433 (5)
H8	0.833562	1.017860	0.987870	0.052*
C9	0.6349 (3)	0.7423 (4)	0.92160 (14)	0.0389 (5)
H9	0.518731	0.748123	0.964163	0.047*
C10	0.6177 (3)	0.5727 (3)	0.84595 (13)	0.0329 (4)
H10	0.490632	0.462217	0.837655	0.039*

Atomic displacement parameters (Å^2)

	U^{11}	U^{22}	U^{33}	U^{12}	U^{13}	U^{23}
N1	0.0313 (7)	0.0251 (7)	0.0323 (7)	−0.0007 (6)	0.0050 (6)	−0.0005 (6)
N2	0.0325 (7)	0.0279 (7)	0.0303 (7)	0.0030 (6)	0.0052 (6)	0.0012 (6)
C1	0.0346 (9)	0.0248 (8)	0.0282 (7)	0.0022 (7)	0.0034 (6)	0.0014 (6)
C2	0.0298 (8)	0.0280 (8)	0.0270 (7)	0.0015 (7)	0.0069 (6)	−0.0028 (7)
C3	0.0330 (9)	0.0236 (8)	0.0321 (8)	0.0014 (7)	0.0082 (6)	0.0003 (6)
C4	0.0287 (9)	0.0344 (10)	0.0360 (8)	0.0025 (7)	0.0045 (7)	−0.0039 (7)
C5	0.0263 (8)	0.0299 (9)	0.0269 (7)	0.0013 (7)	−0.0004 (6)	0.0035 (6)
C6	0.0290 (9)	0.0365 (9)	0.0358 (9)	−0.0019 (8)	0.0033 (7)	0.0060 (7)
C7	0.0398 (11)	0.0341 (9)	0.0443 (10)	−0.0084 (8)	−0.0047 (8)	0.0011 (8)
C8	0.0461 (12)	0.0386 (10)	0.0394 (10)	0.0040 (9)	−0.0052 (8)	−0.0093 (8)
C9	0.0370 (10)	0.0457 (12)	0.0337 (9)	0.0048 (9)	0.0062 (7)	−0.0040 (8)
C10	0.0294 (8)	0.0348 (9)	0.0332 (8)	−0.0019 (7)	0.0033 (6)	0.0008 (7)

Geometric parameters (Å, º)

N1—C1	1.351 (2)	C5—C10	1.391 (3)
N1—N2	1.353 (2)	C5—C6	1.392 (2)
N1—H1N	0.90 (2)	C6—C7	1.384 (3)
N2—C3	1.332 (2)	C6—H6	0.9500
C1—C2	1.378 (3)	C7—C8	1.378 (3)
C1—H1	0.9500	C7—H7	0.9500
C2—C3	1.401 (2)	C8—C9	1.385 (3)
C2—C4	1.500 (2)	C8—H8	0.9500
C3—H3	0.9500	C9—C10	1.388 (3)
C4—C5	1.511 (2)	C9—H9	0.9500
C4—H4A	0.9900	C10—H10	0.9500
C4—H4B	0.9900		
C1—N1—N2	111.63 (14)	C10—C5—C6	118.22 (16)
C1—N1—H1N	130.0 (15)	C10—C5—C4	122.19 (15)
N2—N1—H1N	118.0 (15)	C6—C5—C4	119.55 (16)
C3—N2—N1	104.56 (13)	C7—C6—C5	120.94 (18)
N1—C1—C2	107.75 (15)	C7—C6—H6	119.5
N1—C1—H1	126.1	C5—C6—H6	119.5
C2—C1—H1	126.1	C8—C7—C6	120.44 (19)
C1—C2—C3	103.75 (15)	C8—C7—H7	119.8
C1—C2—C4	128.29 (16)	C6—C7—H7	119.8
C3—C2—C4	127.76 (17)	C7—C8—C9	119.31 (18)
N2—C3—C2	112.30 (15)	C7—C8—H8	120.3
N2—C3—H3	123.8	C9—C8—H8	120.3
C2—C3—H3	123.8	C8—C9—C10	120.38 (18)
C2—C4—C5	116.15 (15)	C8—C9—H9	119.8
C2—C4—H4A	108.2	C10—C9—H9	119.8
C5—C4—H4A	108.2	C9—C10—C5	120.69 (17)
C2—C4—H4B	108.2	C9—C10—H10	119.7
C5—C4—H4B	108.2	C5—C10—H10	119.7
H4A—C4—H4B	107.4		
C1—N1—N2—C3	−0.69 (18)	C2—C4—C5—C6	−143.18 (17)
N2—N1—C1—C2	0.29 (19)	C10—C5—C6—C7	0.6 (3)
N1—C1—C2—C3	0.21 (18)	C4—C5—C6—C7	−177.05 (16)
N1—C1—C2—C4	−174.91 (16)	C5—C6—C7—C8	−0.4 (3)
N1—N2—C3—C2	0.84 (18)	C6—C7—C8—C9	−0.4 (3)
C1—C2—C3—N2	−0.67 (19)	C7—C8—C9—C10	0.9 (3)
C4—C2—C3—N2	174.49 (15)	C8—C9—C10—C5	−0.7 (3)
C1—C2—C4—C5	−112.26 (19)	C6—C5—C10—C9	−0.1 (3)
C3—C2—C4—C5	73.7 (2)	C4—C5—C10—C9	177.52 (16)
C2—C4—C5—C10	39.2 (2)		

Hydrogen-bond geometry (Å, º)

D—H⋯A	D—H	H⋯A	D⋯A	D—H⋯A
N1—H1N⋯N2^i	0.90 (2)	2.01 (2)	2.887 (2)	163 (2)

Symmetry code: (i) −x, y−1/2, −z+1.

3,5-Diamino-4-benzyl-1H-pyrazole (2)

Crystal data

$C_{10}H_{12}N_4$	$F(000) = 400$
$M_r = 188.24$	$D_x = 1.339$ Mg m^{-3}
Monoclinic, $P2_1/c$	Cu $K\alpha$ radiation, $\lambda = 1.54178$ Å
$a = 17.410$ (2) Å	Cell parameters from 7332 reflections
$b = 4.7271$ (7) Å	$\theta = 5.1$–79.3°
$c = 11.4664$ (15) Å	$\mu = 0.69$ mm^{-1}
$\beta = 98.247$ (6)°	$T = 150$ K
$V = 933.9$ (2) Å^3	Block, colourless
$Z = 4$	$0.23 \times 0.21 \times 0.11$ mm

Data collection

Bruker AXS D8 Quest diffractometer	$T_{min} = 0.543$, $T_{max} = 0.754$
Radiation source: I-mu-S 3.0 microsource X-ray tube	10090 measured reflections
	1963 independent reflections
HELIOS multilayer Montel optics monochromator	1817 reflections with $I > 2\sigma(I)$
	$R_{int} = 0.063$
Detector resolution: 7.4074 pixels mm^{-1}	$\theta_{max} = 79.8°$, $\theta_{min} = 5.1°$
ω and phi scans	$h = -22 \rightarrow 21$
Absorption correction: multi-scan (SADABS; Krause *et al.*, 2015)	$k = -5 \rightarrow 5$
	$l = -14 \rightarrow 14$

Refinement

Refinement on F^2	Secondary atom site location: difference Fourier map
Least-squares matrix: full	
$R[F^2 > 2\sigma(F^2)] = 0.038$	Hydrogen site location: mixed
$wR(F^2) = 0.095$	H atoms treated by a mixture of independent and constrained refinement
$S = 1.03$	
1963 reflections	$w = 1/[\sigma^2(F_o^2) + (0.0335P)^2 + 0.2938P]$
142 parameters	where $P = (F_o^2 + 2F_c^2)/3$
0 restraints	$(\Delta/\sigma)_{max} < 0.001$
Primary atom site location: dual	$\Delta\rho_{max} = 0.21$ e Å^{-3}
	$\Delta\rho_{min} = -0.20$ e Å^{-3}

Special details

Geometry. All esds (except the esd in the dihedral angle between two l.s. planes) are estimated using the full covariance matrix. The cell esds are taken into account individually in the estimation of esds in distances, angles and torsion angles; correlations between esds in cell parameters are only used when they are defined by crystal symmetry. An approximate (isotropic) treatment of cell esds is used for estimating esds involving l.s. planes.

Fractional atomic coordinates and isotropic or equivalent isotropic displacement parameters (Å^2)

	x	y	z	U_{iso}*/U_{eq}
N1	0.45388 (5)	0.6148 (2)	0.34503 (8)	0.0242 (2)

N2	0.42688 (6)	0.7374 (2)	0.23732 (8)	0.0244 (2)
H2	0.4576 (9)	0.859 (3)	0.2061 (14)	0.037*
N3	0.39960 (6)	0.2960 (2)	0.47002 (8)	0.0245 (2)
H3A	0.4465 (10)	0.288 (3)	0.5142 (14)	0.037*
H3B	0.3739 (9)	0.129 (4)	0.4651 (14)	0.037*
N4	0.32068 (6)	0.7197 (2)	0.08053 (8)	0.0253 (2)
H4A	0.3421 (9)	0.876 (4)	0.0527 (14)	0.038*
H4B	0.2685 (10)	0.736 (3)	0.0774 (14)	0.038*
C1	0.39646 (6)	0.4405 (2)	0.36362 (9)	0.0214 (2)
C2	0.33394 (6)	0.4435 (2)	0.27059 (9)	0.0215 (2)
C3	0.35673 (6)	0.6383 (2)	0.19157 (9)	0.0218 (2)
C4	0.26130 (6)	0.2683 (2)	0.25826 (9)	0.0240 (2)
H4C	0.273491	0.083850	0.297498	0.029*
H4D	0.244323	0.230743	0.173545	0.029*
C5	0.19460 (6)	0.4035 (2)	0.30979 (9)	0.0241 (2)
C6	0.18121 (7)	0.3371 (3)	0.42321 (10)	0.0302 (3)
H6	0.213624	0.203060	0.468164	0.036*
C7	0.12111 (7)	0.4639 (3)	0.47196 (11)	0.0364 (3)
H7	0.112630	0.415162	0.549475	0.044*
C8	0.07384 (8)	0.6599 (3)	0.40819 (14)	0.0407 (3)
H8	0.033299	0.748953	0.441860	0.049*
C9	0.08595 (8)	0.7262 (3)	0.29431 (15)	0.0450 (4)
H9	0.053343	0.859940	0.249479	0.054*
C10	0.14562 (7)	0.5973 (3)	0.24591 (12)	0.0359 (3)
H10	0.153077	0.642532	0.167597	0.043*

Atomic displacement parameters (Å²)

	U^{11}	U^{22}	U^{33}	U^{12}	U^{13}	U^{23}
N1	0.0249 (5)	0.0267 (5)	0.0216 (4)	0.0011 (4)	0.0054 (4)	0.0021 (3)
N2	0.0252 (5)	0.0264 (5)	0.0225 (4)	−0.0012 (4)	0.0070 (4)	0.0042 (3)
N3	0.0280 (5)	0.0265 (5)	0.0192 (4)	−0.0016 (4)	0.0036 (4)	0.0026 (4)
N4	0.0292 (5)	0.0270 (5)	0.0203 (4)	0.0014 (4)	0.0057 (4)	0.0028 (3)
C1	0.0251 (5)	0.0216 (5)	0.0186 (5)	0.0023 (4)	0.0066 (4)	−0.0020 (4)
C2	0.0247 (5)	0.0220 (5)	0.0187 (5)	0.0010 (4)	0.0061 (4)	−0.0012 (4)
C3	0.0252 (5)	0.0220 (5)	0.0194 (5)	0.0023 (4)	0.0074 (4)	−0.0017 (4)
C4	0.0287 (6)	0.0245 (5)	0.0191 (5)	−0.0031 (4)	0.0044 (4)	−0.0018 (4)
C5	0.0232 (5)	0.0254 (5)	0.0233 (5)	−0.0058 (4)	0.0022 (4)	−0.0024 (4)
C6	0.0301 (6)	0.0383 (6)	0.0222 (5)	−0.0012 (5)	0.0032 (4)	−0.0021 (5)
C7	0.0321 (6)	0.0488 (7)	0.0296 (6)	−0.0066 (5)	0.0090 (5)	−0.0091 (5)
C8	0.0269 (6)	0.0408 (7)	0.0567 (8)	−0.0031 (5)	0.0144 (6)	−0.0124 (6)
C9	0.0302 (7)	0.0403 (7)	0.0649 (10)	0.0055 (5)	0.0080 (6)	0.0119 (7)
C10	0.0306 (6)	0.0392 (7)	0.0381 (7)	0.0000 (5)	0.0062 (5)	0.0115 (5)

Geometric parameters (Å, º)

N1—C1	1.3360 (14)	C4—H4C	0.9900
N1—N2	1.3839 (13)	C4—H4D	0.9900

N2—C3	1.3425 (15)	C5—C10	1.3869 (17)
N2—H2	0.894 (16)	C5—C6	1.3896 (15)
N3—C1	1.3924 (13)	C6—C7	1.3906 (17)
N3—H3A	0.898 (17)	C6—H6	0.9500
N3—H3B	0.905 (17)	C7—C8	1.378 (2)
N4—C3	1.3906 (14)	C7—H7	0.9500
N4—H4A	0.905 (17)	C8—C9	1.388 (2)
N4—H4B	0.907 (17)	C8—H8	0.9500
C1—C2	1.4106 (15)	C9—C10	1.3871 (19)
C2—C3	1.3892 (14)	C9—H9	0.9500
C2—C4	1.5012 (15)	C10—H10	0.9500
C4—C5	1.5174 (15)		
C1—N1—N2	103.56 (9)	C2—C4—H4D	108.7
C3—N2—N1	112.10 (9)	C5—C4—H4D	108.7
C3—N2—H2	129.1 (10)	H4C—C4—H4D	107.6
N1—N2—H2	118.7 (10)	C10—C5—C6	118.05 (11)
C1—N3—H3A	115.6 (10)	C10—C5—C4	121.30 (10)
C1—N3—H3B	114.6 (10)	C6—C5—C4	120.66 (10)
H3A—N3—H3B	113.7 (14)	C5—C6—C7	121.06 (12)
C3—N4—H4A	113.2 (10)	C5—C6—H6	119.5
C3—N4—H4B	112.2 (10)	C7—C6—H6	119.5
H4A—N4—H4B	112.1 (14)	C8—C7—C6	120.20 (12)
N1—C1—N3	120.41 (10)	C8—C7—H7	119.9
N1—C1—C2	112.78 (9)	C6—C7—H7	119.9
N3—C1—C2	126.62 (10)	C7—C8—C9	119.43 (12)
C3—C2—C1	103.77 (9)	C7—C8—H8	120.3
C3—C2—C4	128.31 (10)	C9—C8—H8	120.3
C1—C2—C4	127.88 (10)	C10—C9—C8	120.05 (13)
N2—C3—C2	107.78 (9)	C10—C9—H9	120.0
N2—C3—N4	121.81 (10)	C8—C9—H9	120.0
C2—C3—N4	130.32 (10)	C5—C10—C9	121.20 (12)
C2—C4—C5	114.35 (9)	C5—C10—H10	119.4
C2—C4—H4C	108.7	C9—C10—H10	119.4
C5—C4—H4C	108.7		
C1—N1—N2—C3	−1.02 (11)	C3—C2—C4—C5	−92.03 (13)
N2—N1—C1—N3	−174.26 (9)	C1—C2—C4—C5	90.56 (13)
N2—N1—C1—C2	0.95 (11)	C2—C4—C5—C10	83.88 (13)
N1—C1—C2—C3	−0.55 (12)	C2—C4—C5—C6	−95.73 (12)
N3—C1—C2—C3	174.30 (10)	C10—C5—C6—C7	−0.83 (18)
N1—C1—C2—C4	177.35 (10)	C4—C5—C6—C7	178.80 (11)
N3—C1—C2—C4	−7.80 (17)	C5—C6—C7—C8	−0.36 (19)
N1—N2—C3—C2	0.72 (12)	C6—C7—C8—C9	1.0 (2)
N1—N2—C3—N4	−176.05 (9)	C7—C8—C9—C10	−0.5 (2)
C1—C2—C3—N2	−0.11 (11)	C6—C5—C10—C9	1.34 (19)
C4—C2—C3—N2	−178.00 (10)	C4—C5—C10—C9	−178.28 (12)
C1—C2—C3—N4	176.29 (10)	C8—C9—C10—C5	−0.7 (2)

C4—C2—C3—N4	−1.60 (18)

Hydrogen-bond geometry (Å, º)

D—H···*A*	*D*—H	H···*A*	*D*···*A*	*D*—H···*A*
N2—H2···N1[i]	0.894 (16)	2.108 (16)	2.9912 (13)	169.7 (14)
N3—H3*A*···N1[ii]	0.898 (17)	2.240 (17)	3.1032 (14)	161.0 (13)
N3—H3*B*···N4[iii]	0.905 (17)	2.383 (16)	3.1521 (14)	142.8 (13)
N4—H4*A*···N3[iv]	0.905 (17)	2.140 (18)	3.0388 (14)	171.7 (14)

Symmetry codes: (i) −*x*+1, *y*+1/2, −*z*+1/2; (ii) −*x*+1, −*y*+1, −*z*+1; (iii) *x*, −*y*+1/2, *z*+1/2; (iv) *x*, −*y*+3/2, *z*−1/2.